Published in final edited form as:
Cell. 2012 June 22; 149(7): 1594–1606. doi:10.1016/j.cell.2012.05.018.

The RacGAP β-Chimaerin Selectively Mediates Stereotyped Hippocampal Axonal Pruning

Martin M. Riccomagno[1,3], **Andrés Hurtado**[2,3,6], **HongBin Wang**[4], **Joshua G. J. Macopson**[1,3], **Erin M. Griner**[4], **Andrea Betz**[5], **Nils Brose**[5], **Marcelo G. Kazanietz**[4], and **Alex L. Kolodkin**[1,3]

[1]The Solomon H. Snyder Department of Neuroscience, Howard Hughes Medical Institute

[2]Department of Neurology

[3]The Johns Hopkins University School of Medicine, Baltimore, Maryland 21205, USA.

[4]Department of Pharmacology, Perelman School of Medicine, University of Pennsylvania, Philadelphia, Pennsylvania 19104-6160, USA.

[5]Department of Molecular Neurobiology and DFG Center for Molecular Physiology of the Brain, Max Planck Institute of Experimental Medicine, D-37075 Göttingen, Germany.

[6]International Center for Spinal Cord Injury, Hugo W. Moser Research Institute at Kennedy Krieger, Baltimore, MD 21205, USA.

Summary

Axon pruning and synapse elimination are critical for establishing neural connectivity and synaptic plasticity. Stereotyped pruning of axons that originate in the hippocampal dentate gyrus (DG) and extend in the infrapyramidal tract (IPT) occurs during postnatal murine development by neurite retraction and resembles axon repulsion. The chemorepellent Sema3F is required for IPT axon pruning, dendritic spine remodeling and repulsion of DG axons. However, the signaling events that regulate IPT pruning are not known. We find that inhibition of the small G-protein Rac1 by the Rac GTPase activating protein (GAP) β2-Chimaerin (β2Chn) is essential for Sema3F-mediated IPT pruning. β2Chn selectively binds to the Sema3F receptor neuropilin-2. Sema3F activation of β2Chn is necessary for pruning both *in vitro* and *in vivo*, but is dispensable for axon repulsion and spine remodeling. Therefore, β2Chn contributes to a mechanistic distinction among DG axon pruning, repulsion, and dendritic spine remodeling, all mediated by the repellent Sema3F.

Introduction

Axon pruning events facilitate the removal of ectopic or misguided axons and play key roles in neural circuit formation (Vanderhaeghen and Cheng, 2010). These exuberant axons often form synaptic connections, thus synapse elimination usually precedes pruning (Liu et al., 2005; Low et al., 2008). Disruption of normal pruning events during neural development and circuit maturation is linked to mental illness and brain dysfunction (Johnston, 2004; Lewis and Levitt, 2002; Pardo and Eberhart, 2007; Rapoport et al., 1999). Axon pruning

Corresponding Author: Alex L. Kolodkin kolodkin@jhmi.edu.

events include two classes based on histological findings: degenerative-like axon collateral elimination in which axon fragmentation is observed, and retraction-like pruning whereby axons draw back without shedding membrane fragments (Luo and O'Leary, 2005). Examples of the first class include axon remodeling in the *Drosophila* mushroom body (Lee et al., 1999) and, in mammals, cortical layer 5 axon pruning (Stanfield et al., 1982) and remodeling of retinocollicular axonal projections (McLaughlin et al., 2003; Nikolaev et al., 2009). However, the molecular mechanisms that underlie axon pruning are poorly understood.

A particularly interesting example of retraction-mediated stereotyped pruning involves the hippocampal infrapyramidal tract (IPT), also known as the infrapyramidal bundle (Bagri et al., 2003). During neural development, the IPT extends parallel to the main bundle (MB) of dentate gyrus mossy fibers. While the MB is directed to the apical dendrites of CA3 pyramidal neurons, the IPT axons make synaptic connections with basal dendrites of CA3 pyramidal neurons. During postnatal development, starting between postnatal day 20 (P20) and P30, distal IPT synapses are eliminated and IPT axons retract (Bagri et al., 2003; Liu et al., 2005). Variations in IPT length are correlated with behavioral deficits (Crusio et al., 1987; Lipp et al., 1988) and they accompany an assortment of genetic and environmental influences, including maternal alcohol consumption, perinatal hyperthyroidism and epilepsy (Holmes et al., 1999; Lauder and Mugnaini, 1977; West et al., 1981). IPT pruning is regulated by the secreted semaphoring ligand Sema3F and its receptor complex, comprised of neuropilin 2 (Npn-2) and plexin A3 (PlexA3) proteins (Bagri et al., 2003; Sahay et al., 2003): a signaling pathway well known for serving key roles in CNS and PNS axon guidance events during neural development (Tran et al., 2007). A role for reverse ephrin-B signaling in IPT pruning has also been described (Xu and Henkemeyer, 2009)

Although axon pruning in the vertebrate hippocampus superficially resembles axonal repulsion, the degree of similarity between mechanisms that underlie axon pruning and repulsion remains to be elucidated. For example, do the same cytoplasmic effectors mediate axon pruning and guidance? Here, we show that repulsive axon guidance and stereotypical axonal pruning elicited by the same guidance cue results from the employment of distinct signaling mechanisms, shedding light on fundamental differences between unique modes of inhibitory influences on neuronal processes during postnatal neural development.

Results

Downregulation of RacGTP is Required for IPT Pruning

To investigate the molecular mechanisms underlying hippocampal IPT axon pruning, we first asked whether Rac, a small GTPase with established roles in the regulation of neuronal morphology, axon guidance and actin remodeling (Hall and Lalli, 2010), is modulated by Sema3F. Treatment of DIV14 hippocampal primary neuronal cultures, or a neuroblastoma cell line that expresses Sema3F receptor components (Neuro2A cells; Figure S1A), with 10 nM Sema3F results in a significant decrease in the levels of activated Rac1 (Rac1-GTP) detected in cell lysates, as compared to alkaline phosphatase (AP) control treatment (Figures S1B and S1C; p=0.0031 and p=0.016, for Neuro2A cells and cultured hippocampal neurons, respectively). To assess Sema3F effects on the axonal pool of Rac1-GTP, we performed immunocytochemical detection of Rac/Cdc42-GTP using the PBD domain of PAK1 (Harrington et al., 2011) following Sema3F or AP-control treatments. We observed a striking reduction of activated Rac/Cdc42 in axons when cultured hippocampal neurons were treated with Sema3F (Figures 1A–1C, p=0.0008; Figure S1D). Taken together, these Rho-GTPase pulldown and immunocytochemical assays suggest that Sema3F negatively regulates Rac1-GTP levels.

To determine whether Sema3F-mediated reduction in Rac-GTP levels is required *in vivo* for IPT pruning, we stereotactically injected dentate gyri of P20 mice with lentivirus vectors that encode either a constitutively active form of Rac1 (*RacQL*) under the control of the ubiquitin promoter followed by an internal ribosomal entry site (*IRES*) and *EGFP,* or *EGFP* alone. This strategy results in robust expression of these transgenes in the dentate gyrus and produced strong labeling of most mossy fiber axons at P45 (Figure 1F). IPT pruning occurs normally in mice injected with the control EGFP-expressing lentivirus, with GFP^+ axons in the IPT retracting to 47% of the main mossy fiber bundle length at P45 (Figure 1D). However, GFP^+ IPT axons in hippocampi of mice injected with the *RacQL*- expressing lentivirus extend 78% of the main mossy fiber bundle length at P45 (Figures 1E and 1G). This defect in IPT retraction following expression of RacQL suggests that Rac inhibition is required for IPT pruning. Since previous work shows that synapses are present in the distal unpruned IPT of *Npn2*$^{-/-}$ and *PlexinA3*$^{-/-}$ mutant mice (Liu et al., 2005), we immunostained mice injected with the lentivirus expressing *RacQL* or the control lentivirus with the presynaptic marker vGlut1 to investigate whether Rac inhibition is also required for dissolution of presynaptic specializations. Interestingly, expression of *RacQL* in the dentate gyrus results in strong vGlut1 staining in distal GFP^+ IPT axons that is not observed in *EGFP*-expressing control-injected mice (Figures 1H and 1I). These results suggest Rac inhibition is necessary for the elimination of IPT presynaptic components and axon pruning.

The RacGAP β2-Chimaerin Binds to Npn-2, is Activated by Sema3F and is Expressed in the DG During IPT Pruning

Rho GTPase activating proteins (GAPs) and Rho guanine nucleotide exchange factors (GEFs) play key roles in guidance cue signaling and axonal pruning (Bashaw and Klein, 2010; Billuart et al., 2001). We took a candidate approach to investigate the identity of the Rac-GAPs with the potential to inhibit Rac in response to Sema3F signaling during IPT pruning, and we found that the Rac-GAP β2-Chimaerin (β2Chn) robustly binds to Npn2, the ligand binding component of the Sema3F holo-receptor complex (Figure 2A). We performed co-immunoprecipitation (co-IP) experiments to investigate whether both members of the small chimaerin protein family, α2- or β2-chimaerin, bind to Npn-2. Though α2−chimaerin (αChn) also exhibits binding to Npn-2, it is at least ~5 -fold weaker than β2Chn when normalized to input (Figure 2A and Figure S2A). Weak binding of β2Chn to PlexinA3 was also detected (Figure S2A).

α- and β-Chn share 72% amino acid identity and are expressed in the developing and postnatal CNS (Yang and Kazanietz, 2007). αChn is implicated in axon guidance events downstream of ephrin receptor signaling (Beg et al., 2007; Iwasato et al., 2007; Wegmeyer et al., 2007), influences oculomotor function in humans (Miyake et al., 2008), regulates cortical neuronal migration (Ip et al., 2011) and when overexpressed *in vitro* induces dendritic pruning of dissociated hippocampal neurons (Buttery et al., 2006); however, the role of βChn during neural development is unknown. Since Npn-2 binds robustly to β2Chn, we asked whether Sema3F modulates β2Chn activity. We performed FRET experiments using a previously characterized β2Chn-CFP/Rac1-YFP probe pair that allows for direct assessment of β2Chn activation and recruitment to the cell membrane (Wang et al., 2006) (Figure 2B). Neuro2a cells expressing these fluorescent probes were treated with 10nM Sema3F-AP or AP-control (Figures 2C and 2D). Though addition of control AP ligand elicits no change in FRET, treatment with Sema3F triggers a robust increase in Rac1-β2Chn interaction at the cell membrane ($p<0.0001$) with no change in cytosolic FRET (Figures 2C–2E). These results demonstrate that Sema3F can induce β2Chn activation. To begin to address how Sema3F achieves this, we examined whether Sema3F regulates binding of β2Chn to Npn-2. Bath application of Sema3F onto Neuro2A cells for 20 minutes causes a significant reduction in the association of β2Chn with Npn-2 (Figure 2F), suggesting that

Sema3F activation of β2Chn includes promotion of β2Chn release from Npn-2 to facilitate its activation at the cell membrane.

We next assessed the *βChn* temporal and spatial expression patterns during hippocampal postnatal development using RNA *in situ* hybridization. At early postnatal stages, starting at P1, weak expression of *βChn* is observed in the dentate gyrus. However, transcript levels progressively increase and peak between P20 and P45 (Figure 2G and Figure S2). Thus, the timing of peak *βChn* expression in the dentate gyrus overlaps with IPT pruning.

β-Chimaerin is Required for Downregulation of RacGTP and for Presynaptic Pruning *in vitro*, but is Dispensable for Axon Guidance

To test whether or not βChn, which is encoded by the *Chn2* gene, is required for Sema3F-induced inhibition of RacGTP levels, we performed immunocytochemical detection of activated Rac/Cdc42 on WT and $Chn2^{-/-}$ hippocampal cultures acutely treated with Sema3F (Figures 3A–3D). $Chn2^{-/-}$ hippocampal neurons were derived from a newly generated $Chn2^{-/-}$ null mutant mouse (Figure S3). In contrast to the dramatic reduction in GST-PAK1-PBD staining following Sema3F treatment that we observed in WT cultured hippocampal neurons (Figures 3A, 3B and 3E), $Chn2^{-/-}$ neurons show no decrease in activated Rac/Cdc42 upon Sema3F treatment (Figures 3C–3E). Since βChn is a GAP that acts specifically on Rac and does not affect the GTPase activity of Rho or Cdc42 (Yang and Kazanietz, 2007), our data demonstrate that β2Chn is required for Sema3F-dependent inhibition of Rac-GTP levels and does not significantly affect levels of activated Cdc42.

Is β2Chn required for Sema3F-induced pruning? We used an *in vitro* assay to address this issue. One of the first steps in IPT pruning is the disruption of previously established synaptic connections between dentate gyrus mossy fiber axons and basal dendrites of CA3 pyramidal neurons (Liu et al., 2005). To assess synapse elimination, we used the presynaptic marker synaptoporin (SOP), which specifically labels mature synaptic connections between granule cells and CA3 pyramidal neurons (Grosse et al., 1998). This allowed us to monitor the dissolution of DG/CA3 synapses under different conditions *in vitro* in order to assess synapse integrity. Bath application of Sema3F onto WT dissociated cultured hippocampal neurons (21 DIV) for 24 hrs caused a ~50% decrease in SOP puncta, as compared to control treatment ($p<0.01$; Figures 3F, 3G and 3J). Although the vast majority of SOP puncta are co-localized with mossy fiber boutons (Grosse et al., 1998), a small subset of SOP puncta are associated with inhibitory synapses (Williams et al., 2011) (~25%, Figure S4A; data not shown). However, by co-staining with vGlut1 we confirmed that Sema3F acts mainly to eliminate excitatory SOP^{+};$vGlut1^{+}$ synapses, observing that the decrease we see in total SOP^{+} puncta can be attributed to the decrease $SOP^{+}/vGlut1^{+}$ puncta (AP: 100±10.14%, Sema3F:40.52±5.65%, $p=9.43\times x10^{-6}$; Figures S4A–S4F). In contrast, Sema3F treatment of $Chn2^{-/-}$ hippocampal neurons in culture had no effect on the number of SOP puncta, showing that β2Chn is required for Sema3F-induced elimination of granule cell MF/CA3 pyramidal neuron synapses *in vitro* (Figures 3H–3J).

β2Chn functions *in vitro* to mediate Sema3F-dependent presynaptic pruning, however is it required for Sema3F-dependent repulsive guidance? To address this question, we cultured P2 DG explants from WT mice, which maintain expression of *β2Chn in vitro* (Figures S4G and S4H), and from $Chn2^{-/-}$ mice on alternating stripes of control and Sema3F-AP, or AP control only (Figures 3K–3N). Control stripes had no effect on neurites extending from WT or $Chn2^{-/-}$ DG explants (Figures 3K and 3M). Interestingly, both WT and $Chn2^{-/-}$ axons steered away from Sema3F-AP stripes and extended primarily along the control stripes (Figures 3L and 3N). This shows that β2Chn is dispensable for Sema3F-dependent repulsive axon guidance, establishing that synaptic pruning and repulsive guidance *in vitro* are distinct with respect to a requirement for β2Chn. We also asked whether β2Chn affects sensitivity to

Sema3F in neurite outgrowth assays by culturing WT and *Chn2*$^{-/-}$ DG explants in the presence of Sema3F-AP or AP control ligand. Consistent with our stripe assays, 10 nM Sema3F-AP strongly inhibited neurite outgrowth of both WT and *Chn2*$^{-/-}$ DG explants (Figure 3O and Figures S4I–S4M). Only at a 10-fold lower concentration did Sema3F exert a somewhat stronger inhibitory effect on neurite outgrowth on WT, as compared to *Chn2*$^{-/-}$, neurites (p=0.015, Figure S4M). Taken together, these results show that β2Chn is required for Sema3F-dependent presynaptic pruning but is not essential for Sema3F-mediated DG axon repulsion.

β-Chimaerin is Required and is Sufficient for IPT Pruning

Sema3F, Npn-2 and PlexA3 are required *in vivo* for in IPT pruning (Bagri et al., 2003; Sahay et al., 2003). Therefore, we next asked whether β2Chn is necessary for this developmental process. We performed histological analysis of WT and *Chn2*$^{-/-}$ P45 hippocampi. Timm and anti-calbindin staining show that by P45 the IPT of WT mice is pruned to 51% of the main mossy fiber bundle length (Figures 4A, 4C and 4E; Figures S5A and S5A'). However, the IPT of *Chn2*$^{-/-}$ mice fails to be pruned, remaining 87% the length of the MB (Figures 4B, 4D and 4E; Figures S5B and S5B'; phenotype observed with full penetrance and expressivity). We next asked if presynaptic terminals were still present in the distal region of the *Chn2*$^{-/-}$ unpruned IPT by immunostaining for the presynpatic marker vGlut1. Although WT mice did not exhibit vGlut1^{+} terminals at the distal portion of the region from where the IPT was pruned, abundant vGlut1^{+} puncta are found in the infrapyramidal region near the distal portion of the unpruned IPT mossy fibers in *Chn2*$^{-/-}$ mice (Figures 4C and 4D), suggesting a defect in synaptic pruning. To confirm that β2Chn is required for IPT synaptic pruning, we analyzed the distal infrapyramidal region of WT and *Chn2*$^{-/-}$ mice using transmission electron microscopy (TEM) and quantified the number of synapses in this region (Figures 4F–4H). Consistent with the perdurance of vGlut1 staining we observe in distal unpruned *Chn2*$^{-/-}$ IPT axons, TEM analysis of *Chn2*$^{-/-}$ mice revealed a significant increase in the number of synapses in the distal infrapyramidal region of CA3 as compared to WT (Figures 4F–4H, p=0.005). Similarities in synaptic pruning phenotypes observed in *Chn2*$^{-/-}$ and *Npn2*$^{-/-}$ animals are restricted to DG IPT connections onto CA3 neurons, since we find that the number of spines along DG granule cell dendrities, which is significantly increased in *Npn2*$^{-/-}$ and *Sema3F*$^{-/-}$ mice (Tran et al., 2009), is equivalent to WT in *Chn2*$^{-/-}$ mice (Figures 4I–4K). Furthermore, *Chn2*$^{-/-}$ null mutant mice do not show the embryonic trochlear and oculomotor nerve axon guidance defects, or the late embryonic-postnatal anterior commissure phenotypes, observed in *Npn2*$^{-/-}$ mice (Figures S5C–S5F) (Chen et al., 2000; Giger et al., 2000). Thus, *Chn2* is selectively required for Sema3F-mediated IPT pruning, but not for Npn-2–dependent axon guidance or dendritic spine remodeling.

Our analysis of *Chn2*$^{-/-}$ mice demonstrates a requirement for β2Chn in IPT synaptic pruning and axon retraction. To determine whether β2Chn acts in an instructive fashion to enhance IPT pruning, we took advantage of a newly generated knock-in mouse that harbors an allele of *Chn2* encoding a hyperactive form of βChn; this allele consists of a single amino acid change that has been introduced into the endogenous *Chn2* locus (Figure S6). This I130A point mutation causes the βChn protein to remain in an "open" conformation, rendering the protein more sensitive to induction and, thus, hyperactive (Canagarajah et al., 2004). Since *Chn2*^{I130A} mice produce Chn2 protein that is more easily induced but not constitutively active (Canagarajah et al., 2004; Yang and Kazanietz, 2007), we asked whether or not this mutation when homozygous enhanced pruning at P28, a postnatal time that is well after the onset of IPT pruning but prior to its completion. At P28, the length of the WT IPT is 66% of the MB length (Figures 5A and 5C). This is in contrast to the IPT in *Chn2*$^{I130A/I130A}$ mice, in which the IPT is significantly shorter at this same postnatal time

point (49% of the MB length; Figures 5B and 5C). Importantly, the lengths of WT and *Chn2*$^{I130A/I130A}$ IPTs are not significantly different prior to the onset of pruning at P15 (Figures S6G–S6I). These results show that a hyperactive βChn allele enhances IPT pruning.

The IPT pruning defects observed in *Chn2*$^{-/-}$ mice closely resemble those observed in *Npn-2*$^{-/-}$, *PlexA3*$^{-/-}$, and *Sema3F*$^{-/-}$ hippocampi (Bagri et al., 2003; Liu et al., 2005; Sahay et al., 2003). We obtained additional evidence that *Npn-2* and *Chn2* act in concert during IPT development from an analysis of single and compound heterozygous mutant mice. Histological examination of *Chn2*$^{+/-}$ and *Npn-2*$^{+/-}$ mice revealed that the IPT length in either single heterozygote is indistinguishable from WT at P45 (Figures 5D and 5E). However, transheterozygous *Chn2*$^{+/-}$; *Npn-2*$^{+/-}$ P45 mice exhibit a significant increase in IPT length, as compared to WT ($p<0.01$, Figures 5D and 5E), phenocopying *Chn2*$^{-/-}$ and *Npn-2*$^{-/-}$ single homozygous null mutants (Bagri et al., 2003) (Figure 4B). This robust genetic interaction *in vivo*, combined with our biochemical observations, strongly suggest that Sema3F, Npn-2 and β2Chn function in a common pathway to regulate IPT pruning.

DG-autonomous Requirement for β2-Chimaerin and its GAP Activity During IPT Pruning

To ask whether βChn is indeed required in DG granule cells to mediate IPT pruning, a series of short hairpin RNAs (shRNAs) were generated using the pLEMPRA system (Zhou et al., 2006) to knock down *Chn2* cell-type autonomously in DG granule cells. Two of several shRNAs tested (*shRNA2* and *shRNA4*) elicited significant down-regulation of β2Chn expression (Figure S7; data not shown). *shRNA2* is predicted to anneal to and down-regulate transcripts encoding only one of the two known βChn isoforms, β2Chn (which contains the SH2 domain), however *shRNA4* down regulates the expression of transcripts encoding both the β1Chn isoform (which does not contain the SH2 domain) and the β2Chn isoform (Yang and Kazanietz, 2007). We generated lentiviruses that express both *shRNA2* and *shRNA4*, stereotactically injected them into the DG at P20, and then analyzed the IPT at P45 (Figure 1F). Injection of an EGFP-expressing control lentivirus had no effect on IPT pruning (Figures 6A and 7C). Injection of lentiviruses expressing either *shRNA2* or *shRNA4*, however, resulted in a robust GFP^{+} IPT pruning defect ($p<0.01$; Figures 6B, 6C and 7C). Therefore, βChn is required in DG granule cells to regulate IPT pruning. Further, these results also confirm that the isoform of βChn essential for IPT pruning is β2Chn; *shRNA2* only knocks-down β2Chn, however *shRNA4* knocks-down both isoforms of *βChn*, and we find that both shRNAs elicit the same infrapyramidal tract pruning defect (Figures 6B, 6C and 7C). To rule out the possibility that these defects observed in *shRNA2*-injected animals are due to off-target shRNA effects, and also to show that this shRNA acts specifically to silence *β2Chn*, we generated a pLempra rescue construct that expresses both *shRNA2* and the WT human form of *β2Chn* (*WT**), which is insensitive to *shRNA2* (Figure S7). Injection of the *shRNA2*+*WT** lentivirus completely rescues the IPT pruning phenotype observed in *shRNA2*-injected animals (Figures 7A and 7C), demonstrating that *shRNA2* acts specifically on *β2Chn*, and that β2Chn is required for IPT axon pruning.

Analysis of *Chn2*$^{-/-}$ mice revealed a requirement for β2Chn in IPT axonal and presynaptic pruning. To investigate whether βChn is required in DG granule cells for dissolution of IPT synaptic specializations, we performed vGlut1 immunostaining of control, *shRNA2* and *shRNA4* injected hippocampi (Figures 6D–6F). Indeed, vGlut1 staining is absent from the distal infrapyramidal region of mossy fibers in control EGFP-expressing lentivirus-injected animals (Figure 6D). However, both *shRNA2* and *shRNA4*-injected animals show strong vGlut1immunolabeling on distal GFP^{+} IPT axons (Figures 6E and 6F), showing that βChn is required in DG granule cells to regulate IPT mossy fiber presynaptic elimination. Injection of *shRNA2*+*WT** lentivirus completely rescues the perdurance of the presynaptic marker vGlut1 observed in *shRNA2*-injected animals (Figures 6E and 7D), further confirming the

specificity of the *shRNA2* knock-down and the requirement for β2Chn in IPT axon and presynaptic pruning.

We observe that Sema3F down-regulates Rac-GTP in DG neurons and that constitutively active Rac blocks IPT pruning *in vivo* (Figure 1). In addition, our *in vitro* observations using *Chn2*$^{-/-}$ neuronal cultures show that β2Chn is required for Sema-3F–mediated down regulation of Rac-GTP (Figures 3A–3E). These observations suggest that β2Chn Rac-GAP activity is required for IPT pruning. To test this hypothesis, we generated a pLempra rescue construct expressing human β2Chn (which is insensitive to *shRNA2*) that harbors a micro-deletion in the β2Chn GAP domain rendering it inactive (Siliceo et al., 2006) (*shRNA2*+Δ*EIE**; Figure S7). Expression levels of *shRNA2*+*WT** and *shRNA2*+Δ*EIE** lentiviruses are similar (Figure S7). In contrast to the complete rescue observed when *shRNA2*+*WT** lentivirus was injected into the DG, *shRNA2*+Δ*EIE**-injected animals exhibited exuberantly extended GFP^{+} IPT axons that were significantly longer than the IPTs of control- or *shRNA2*+*WT**-injected animals ($p<0.01$, Figures 6A and 7A–7C). Closer examination of distal GFP^{+} IPT fibers in *shRNA2* + *ΔEIE**-injected animals revealed extensive vGlut1 immunostaining (Figure 7E), indicating that presynaptic elimination also requires an active β2Chn GAP domain. These results show that β2Chn Rac-GAP activity is required *in vivo* for IPT presynaptic elimination and axon pruning.

Discussion

We demonstrate here that Sema3F-dependent inhibition of Rac1 by the Rac-GAP β2Chn is required for hippocampal infrapyramidal tract pruning. Axon pruning, together with other neural developmental processes including axon guidance, synapse remodeling and dendritic spine elimination, play essential roles during the establishment of functional brain circuitry (Vanderhaeghen and Cheng, 2010). Although little is known about the signaling pathways that regulate axon pruning, recent studies have uncovered mechanisms that regulate degenerative-like axon elimination, highlighting the importance of signaling pathways previously shown to mediate controlled cell death (Nikolaev et al., 2009), proteasome-mediated degradation (Watts et al., 2003) and Wallerian degeneration (Hoopfer et al., 2006). Our observations provide insight into the molecular mechanisms that regulate stereotyped retraction-mediated axon pruning. They support a novel role for Sema3F-mediated activation of the Rac-GAP β2Chn in stereotyped axon pruning and synapse elimination in the IPT, a hippocampal tract implicated in spatial memory and avoidance learning (Crusio et al., 1987; Lipp et al., 1988).

RhoGTPase-mediated Signaling and Stereotyped Axon Pruning

Our data support a model in which Sema3F signaling activates a RacGAP in order to downregulate RacGTP levels, thereby promoting presynaptic remodeling and axon pruning. Treatment of hippocampal neuronal cultures with Sema3F causes a significant decrease in axonal RacGTP levels. Overexpressing a constitutively-active form of Rac prior to the onset of IPT pruning results in a lack of IPT axon retraction and synapse elimination, revealing that downregulation of RacGTP is critical for IPT pruning *in vivo*. While Rac inhibition by Sema3F is required *in vitro* and *in vivo* for hippocampal IPT pruning, ephrin reverse signaling, which is essential for IPT pruning *in vivo*, activates Rac1 *in vitro* by recruiting the adaptor protein Grb4 and the RacGEF Dock180 (Xu and Henkemeyer, 2009). This raises the possibility that tight temporal and spatial regulation of Rac activation and inactivation, provided by opposing activities of Sema3F and ephrin-reverse signaling, may be important for IPT pruning. Assessment of crosstalk between these two signaling pathways *in vivo* will further our understanding of the molecular mechanisms that underlie IPT pruning. Whether regulation of Rho GTPases is a common feature of retraction-like and degradation-mediated pruning remains to be elucidated. In that regard, p190RhoGAP is required for the regulation

of mushroom body remodeling in Drosophila (Billuart et al., 2001), a degeneration-like pruning event, and this raises the possibility that these two classes of pruning, although superficially distinct, may share common molecular mechanisms. Future experiments will determine whether similar signaling events underlie other classes of axon pruning in mammals.

How does Sema3F regulate β2Chn activity? Genetic and biochemical evidence suggest that Npn-2 and β2Chn act in concert to direct IPT pruning. Interestingly, Sema3F promotes dissociation of β2Chn from Npn-2 in a dose-dependent manner. One plausible scenario is that Sema signaling acts in a sequential, ligand-gated, manner to regulate β2Chn activation. Npn-2 recruits and sequesters β2Chn in relevant areas of the cell, for example in close proximity to the axonal membrane. Sema3F binding to Npn-2 then promotes the release of β2Chn, which initiates pruning through subsequent recruitment to the membrane and activation.

Semaphorin signaling is essential for IPT pruning and the synapse elimination events that precede it (Liu et al., 2005). Histological evidence reveals that in *Npn-2*$^{-/-}$ and *PlexA3*$^{-/-}$ mice synapse elimination and IPT pruning do not occur, since exuberant axons and synaptic terminals remain in the distal IPT region of these mutants (Liu et al., 2005). We find that β2Chn function and downregulation of RacGTP are also required for both of these developmental processes. It remains to be seen whether synapse elimination and IPT axonal pruning are two distinct and sequential cellular events, or if both developmental processes are intrinsically linked and controlled by the same molecular mechanisms. Since *Chn2*, *Sema3F*, *Npn-2*, and *PlexA3* mouse null mutants show defects in IPT axon pruning and synapse elimination (Liu et al., 2005) (Figure 4), it seems likely that both events are tightly coupled and regulated in a similar fashion.

Unbalanced synaptic and axonal pruning is implicated in the etiology of mental illness (Johnston, 2004; Lewis and Levitt, 2002; Pardo and Eberhart, 2007; Rapoport et al., 1999; Vanderhaeghen and Cheng, 2010). Improper regulation of axon and synaptic pruning in the cortex, cerebellum and limbic system is correlated with increases in white matter and has been linked to epilepsy and autism (Johnston, 2004;Pardo and Eberhart, 2007; Vanderhaeghen and Cheng, 2010). Furthermore, excessive cortical neurite and synaptic pruning during puberty is correlated with the early onset of schizophrenia (Lewis and Levitt, 2002; Rapoport et al., 1999). Interestingly, a missense polymorphism identified in the human gene that encodes βChn that results in the change of a highly conserved histidine residue to arginine (H204R) is genetically linked to schizophrenia (Hashimoto et al., 2005). Future experiments will address whether βChn plays any role in the etiology of schizophrenia and related disorders.

Selective Requirement for β2Chn During Axonal Pruning

It is intriguing that although β2Chn is required for Sema3F-dependent IPT pruning, this RacGAP is apparently dispensable for Sema3F-mediated DG axon repulsion and dendritic spine remodeling. Indeed, *β2Chn* mutants do not exhibit any of the axon guidance or dendritic morphology defects associated with null mutations in *Sema3F*, *Npn-2*, or *PlexA3* (Figure S5; data not shown) (Chen et al., 2000; Giger et al., 2000; Sahay et al., 2003; Tran et al., 2009). β2Chn may confer unique signaling properties required for pruning by increasing the “gain”, or sensitivity, of granule cell axons to Sema3F signaling involving the same signaling pathways required for regulating neuronal morphology and process guidance. Alternatively, β2Chn may activate signaling pathways that are vital for Sema3F-mediated axon pruning but are distinct from those utilized by Sema3F-mediated axonal repulsion and dendritic spine remodeling. Rather than exclusive utilization of one particular signaling pathway, a balance between different regulators may be required for distinct neuronal

responses to extrinsic cues. The differential requirement for β2Chn in axon pruning, but not axon guidance or dendritic spine remodeling, is one of the first mechanistic distinctions identified among these three developmental inhibitory processes: all mediated in this case by the same guidance cue. Determining the signaling context in which Rho GTPase regulation governs axon pruning, and whether neuronal process pruning and synapse elimination in other neural systems utilize similar mechanisms to sculpt mature neural circuits, will shed light on the underlying mechanisms that participate in neuronal remodeling.

Experimental Procedures

Generation of Transgenic Animals

The mouse line carrying a targeted deletion for *β2-chimaerin (Chn2*$^{-/-}$*)* was generated using the KO-vector pFlexHR (Schnutgen et al., 2003) and results in the abrogation of β2-chimaerin protein expression with concomitant expression of a LacZ cassette under the control of the *Chn2* gene promoter (Figure S3). The knock-in mouse carrying the hyperactive mutant *I130A-β2-chimaerin* was generated using the targeting vector pTKNeoLox (Fernandez-Chacon et al., 2001).

Stereotactic Injection of Lentiviruses

Concentrated viral solution (1 μl), prepared as previously described (Lois et al., 2002), was delivered into the DG by stereotactic injection (0.25 μl per min). For P20 mice, we used the following coordinates: anterior-posterior, −2.1 mm; lateral, ±1.7 mm; and vertical, −1.9 mm. For all injections, Bregma was the reference point.

Fluorescence Resonance Energy Transfer (FRET)

Neuro-2a cells were transfected with CFP-Rac1 (wild type) and YFP-β2-chimaerin (wild type) using Metafectene® PRO (Biontex, Germany); serum-free and phenol-red free medium (10 mM Hepes) was added 24 h after transfection. Images (exposures of 500 ms) were taken every 6s after the addition of either Sema3F (10 nM) or AP (10 nM) and FRET analysis was performed as previously described (Wang et al., 2006).

Statistical Analysis

Quantitation of IPT retraction was performed using the ratio of IPT length to the length of the MB. IPT and MB length was measured from the tip of the inferior blade of the dentate granule cell layer, as reported previously (Bagri et al., 2003). Statistical differences for mean values between two samples were determined by two-tailed Student’s t-test for independent samples. Statistical analyses among multiple groups were determined using ANOVA followed by Tukey's multiple comparison test. The criterion for statistical significance was set at $p < 0.05$.

Tissue Culture and Immunohistochemistry

Hippocampal neuronal cultures were generated as previously described (Tran et al., 2009). Immunohistochemistry and in situ hybridization were performed as previously described (Giger et al., 2000).

Extended Experimental Procedures are available online as Supplementary Material.

Supplementary Material

Refer to Web version on PubMed Central for supplementary material.

Acknowledgments

We thank Dr. Silvio Gutkind for the *RacQL* construct, Barbara Smith and the JHU School of Medicine Microscope Facility for assistance with the TEM, and Dr. Michael Greenberg for the pLLX and pLempra vectors. We also thank Drs. Cynthia Duggan, Roman Giger, David Ginty, Randal Hand, Kang Shen and Marc Tessier-Lavigne for helpful comments on the manuscript and discussions, and members of Kolodkin laboratory for assistance. This work was supported by a postdoctoral fellowship from the National Ataxia Foundation to M.M.R,; NIH R01 CA74197 to M.G.K, and NIH RO1 MH59199 to A.L.K.. A.L.K. is an investigator of the Howard Hughes Medical Institute.

References

Bagri A, Cheng HJ, Yaron A, Pleasure SJ, Tessier-Lavigne M. Stereotyped pruning of long hippocampal axon branches triggered by retraction inducers of the semaphorin family. Cell. 2003; 113:285–299. [PubMed: 12732138]

Bashaw GJ, Klein R. Signaling from axon guidance receptors. Cold Spring Harb Perspect Biol. 2010; 2:a001941. [PubMed: 20452961]

Beg AA, Sommer JE, Martin JH, Scheiffele P. alpha2-Chimaerin is an essential EphA4 effector in the assembly of neuronal locomotor circuits. Neuron. 2007; 55:768–778. [PubMed: 17785183]

Billuart P, Winter CG, Maresh A, Zhao X, Luo L. Regulating axon branch stability: the role of p190 RhoGAP in repressing a retraction signaling pathway. Cell. 2001; 107:195–207. [PubMed: 11672527]

Buttery P, Beg AA, Chih B, Broder A, Mason CA, Scheiffele P. The diacylglycerol-binding protein alpha1-chimaerin regulates dendritic morphology. Proc Natl Acad Sci U S A. 2006; 103:1924–1929. [PubMed: 16446429]

Canagarajah B, Leskow FC, Ho JY, Mischak H, Saidi LF, Kazanietz MG, Hurley JH. Structural mechanism for lipid activation of the Rac-specific GAP, beta2-chimaerin. Cell. 2004; 119:407–418. [PubMed: 15507211]

Chen H, Bagri A, Zupicich JA, Zou Y, Stoeckli E, Pleasure SJ, Lowenstein DH, Skarnes WC, Chedotal A, Tessier-Lavigne M. Neuropilin-2 regulates the development of selective cranial and sensory nerves and hippocampal mossy fiber projections. Neuron. 2000; 25:43–56. [PubMed: 10707971]

Crusio WE, Schwegler H, Lipp HP. Radial-maze performance and structural variation of the hippocampus in mice: a correlation with mossy fibre distribution. Brain Res. 1987; 425:182–185. [PubMed: 3427419]

Fernandez-Chacon R, Konigstorfer A, Gerber SH, Garcia J, Matos MF, Stevens CF, Brose N, Rizo J, Rosenmund C, Sudhof TC. Synaptotagmin I functions as a calcium regulator of release probability. Nature. 2001; 410:41–49. [PubMed: 11242035]

Giger RJ, Cloutier JF, Sahay A, Prinjha RK, Levengood DV, Moore SE, Pickering S, Simmons D, Rastan S, Walsh FS, et al. Neuropilin-2 is required in vivo for selective axon guidance responses to secreted semaphorins. Neuron. 2000; 25:29–41. [PubMed: 10707970]

Grosse G, Tapp R, Wartenberg M, Sauer H, Fox PA, Grosse J, Gratzl M, Bergmann M. Prenatal hippocampal granule cells in primary cell culture form mossy fiber boutons at pyramidal cell dendrites. J Neurosci Res. 1998; 51:602–611. [PubMed: 9512004]

Hall A, Lalli G. Rho and Ras GTPases in axon growth, guidance, and branching. Cold Spring Harb Perspect Biol. 2010; 2:a001818. [PubMed: 20182621]

Harrington AW, St Hillaire C, Zweifel LS, Glebova NO, Philippidou P, Halegoua S, Ginty DD. Recruitment of actin modifiers to TrkA endosomes governs retrograde NGF signaling and survival. Cell. 2011; 146:421–434. [PubMed: 21816277]

Hashimoto R, Yoshida M, Kunugi H, Ozaki N, Yamanouchi Y, Iwata N, Suzuki T, Kitajima T, Tatsumi M, Kamijima K. A missense polymorphism (H204R) of a Rho GTPase-activating protein, the chimerin 2 gene, is associated with schizophrenia in men. Schizophr Res. 2005; 73:383–385. [PubMed: 15653288]

Holmes GL, Sarkisian M, Ben-Ari Y, Chevassus-Au-Louis N. Mossy fiber sprouting after recurrent seizures during early development in rats. J Comp Neurol. 1999; 404:537–553. [PubMed: 9987996]

Hoopfer ED, McLaughlin T, Watts RJ, Schuldiner O, O'Leary DD, Luo L. Wlds protection distinguishes axon degeneration following injury from naturally occurring developmental pruning. Neuron. 2006; 50:883–895. [PubMed: 16772170]

Ip JP, Shi L, Chen Y, Itoh Y, Fu WY, Betz A, Yung WH, Gotoh Y, Fu AK, Ip NY. alpha2-chimaerin controls neuronal migration and functioning of the cerebral cortex through CRMP-2. Nat Neurosci. 2011; 15:39–47. [PubMed: 22138645]

Iwasato T, Katoh H, Nishimaru H, Ishikawa Y, Inoue H, Saito YM, Ando R, Iwama M, Takahashi R, Negishi M, et al. Rac-GAP alpha-chimerin regulates motor-circuit formation as a key mediator of EphrinB3/EphA4 forward signaling. Cell. 2007; 130:742–753. [PubMed: 17719550]

Johnston MV. Clinical disorders of brain plasticity. Brain Dev. 2004; 26:73–80. [PubMed: 15036425]

Lakso M, Pichel JG, Gorman JR, Sauer B, Okamoto Y, Lee E, Alt FW, Westphal H. Efficient in vivo manipulation of mouse genomic sequences at the zygote stage. Proc Natl Acad Sci U S A. 1996; 93:5860–5865. [PubMed: 8650183]

Lauder JM, Mugnaini E. Early hyperthyroidism alters the distribution of mossy fibres in the rat hippocampus. Nature. 1977; 268:335–337. [PubMed: 887162]

Lee T, Lee A, Luo L. Development of the Drosophila mushroom bodies: sequential generation of three distinct types of neurons from a neuroblast. Development. 1999; 126:4065–4076. [PubMed: 10457015]

Lewis DA, Levitt P. Schizophrenia as a disorder of neurodevelopment. Annu Rev Neurosci. 2002; 25:409–432. [PubMed: 12052915]

Lipp HP, Schwegler H, Heimrich B, Driscoll P. Infrapyramidal mossy fibers and two-way avoidance learning: developmental modification of hippocampal circuitry and adult behavior of rats and mice. J Neurosci. 1988; 8:1905–1921. [PubMed: 3385481]

Liu XB, Low LK, Jones EG, Cheng HJ. Stereotyped axon pruning via plexin signaling is associated with synaptic complex elimination in the hippocampus. J Neurosci. 2005; 25:9124–9134. [PubMed: 16207871]

Lois C, Hong EJ, Pease S, Brown EJ, Baltimore D. Germline transmission and tissue-specific expression of transgenes delivered by lentiviral vectors. Science. 2002; 295:868–872. [PubMed: 11786607]

Low LK, Liu XB, Faulkner RL, Coble J, Cheng HJ. Plexin signaling selectively regulates the stereotyped pruning of corticospinal axons from visual cortex. Proc Natl Acad Sci U S A. 2008; 105:8136–8141. [PubMed: 18523013]

Luo L, O'Leary DD. Axon retraction and degeneration in development and disease. Annu Rev Neurosci. 2005; 28:127–156. [PubMed: 16022592]

McLaughlin T, Torborg CL, Feller MB, O'Leary DD. Retinotopic map refinement requires spontaneous retinal waves during a brief critical period of development. Neuron. 2003; 40:1147–1160. [PubMed: 14687549]

Miyake N, Chilton J, Psatha M, Cheng L, Andrews C, Chan WM, Law K, Crosier M, Lindsay S, Cheung M, et al. Human CHN1 mutations hyperactivate alpha2-chimaerin and cause Duane's retraction syndrome. Science. 2008; 321:839–843. [PubMed: 18653847]

Nikolaev A, McLaughlin T, O'Leary DD, Tessier-Lavigne M. APP binds DR6 to trigger axon pruning and neuron death via distinct caspases. Nature. 2009; 457:981–989. [PubMed: 19225519]

Pardo CA, Eberhart CG. The neurobiology of autism. Brain Pathol. 2007; 17:434–447. [PubMed: 17919129]

Rapoport JL, Giedd JN, Blumenthal J, Hamburger S, Jeffries N, Fernandez T, Nicolson R, Bedwell J, Lenane M, Zijdenbos A, et al. Progressive cortical change during adolescence in childhood-onset schizophrenia. A longitudinal magnetic resonance imaging study. Arch Gen Psychiatry. 1999; 56:649–654. [PubMed: 10401513]

Sahay A, Molliver ME, Ginty DD, Kolodkin AL. Semaphorin 3F is critical for development of limbic system circuitry and is required in neurons for selective CNS axon guidance events. J Neurosci. 2003; 23:6671–6680. [PubMed: 12890759]

Schnutgen F, Doerflinger N, Calleja C, Wendling O, Chambon P, Ghyselinck NB. A directional strategy for monitoring Cre-mediated recombination at the cellular level in the mouse. Nat Biotechnol. 2003; 21:562–565. [PubMed: 12665802]

Siliceo M, Garcia-Bernal D, Carrasco S, Diaz-Flores E, Coluccio Leskow F, Teixido J, Kazanietz MG, Merida I. Beta2-chimaerin provides a diacylglycerol-dependent mechanism for regulation of adhesion and chemotaxis of T cells. J Cell Sci. 2006; 119:141–152. [PubMed: 16352660]

Stanfield BB, O'Leary DD, Fricks C. Selective collateral elimination in early postnatal development restricts cortical distribution of rat pyramidal tract neurones. Nature. 1982; 298:371–373. [PubMed: 6178041]

Tran TS, Kolodkin AL, Bharadwaj R. Semaphorin regulation of cellular morphology. Annu Rev Cell Dev Biol. 2007; 23:263–292. [PubMed: 17539753]

Tran TS, Rubio ME, Clem RL, Johnson D, Case L, Tessier-Lavigne M, Huganir RL, Ginty DD, Kolodkin AL. Secreted semaphorins control spine distribution and morphogenesis in the postnatal CNS. Nature. 2009; 462:1065–1069. [PubMed: 20010807]

Vanderhaeghen P, Cheng HJ. Guidance molecules in axon pruning and cell death. Cold Spring Harb Perspect Biol. 2010; 2:a001859. [PubMed: 20516131]

Wang H, Yang C, Leskow FC, Sun J, Canagarajah B, Hurley JH, Kazanietz MG. Phospholipase Cgamma/diacylglycerol-dependent activation of beta2-chimaerin restricts EGF-induced Rac signaling. Embo J. 2006; 25:2062–2074. [PubMed: 16628218]

Watts RJ, Hoopfer ED, Luo L. Axon pruning during Drosophila metamorphosis: evidence for local degeneration and requirement of the ubiquitin-proteasome system. Neuron. 2003; 38:871–885. [PubMed: 12818174]

Wegmeyer H, Egea J, Rabe N, Gezelius H, Filosa A, Enjin A, Varoqueaux F, Deininger K, Schnutgen F, Brose N, et al. EphA4-dependent axon guidance is mediated by the RacGAP alpha2-chimaerin. Neuron. 2007; 55:756–767. [PubMed: 17785182]

West JR, Hodges CA, Black AC Jr. Prenatal exposure to ethanol alters the organization of hippocampal mossy fibers in rats. Science. 1981; 211:957–959. [PubMed: 7466371]

Williams ME, Wilke SA, Daggett A, Davis E, Otto S, Ravi D, Ripley B, Bushong EA, Ellisman MH, Klein G, et al. Cadherin-9 regulates synapse-specific differentiation in the developing hippocampus. Neuron. 2011; 71:640–655. [PubMed: 21867881]

Xu NJ, Henkemeyer M. Ephrin-B3 reverse signaling through Grb4 and cytoskeletal regulators mediates axon pruning. Nat Neurosci. 2009; 12:268–276. [PubMed: 19182796]

Yang C, Kazanietz MG. Chimaerins: GAPs that bridge diacylglycerol signalling and the small G-protein Rac. Biochem J. 2007; 403:1–12. [PubMed: 17346241]

Zhou Z, Hong EJ, Cohen S, Zhao WN, Ho HY, Schmidt L, Chen WG, Lin Y, Savner E, Griffith EC, et al. Brain-specific phosphorylation of MeCP2 regulates activity-dependent Bdnf transcription, dendritic growth, and spine maturation. Neuron. 2006; 52:255–269. [PubMed: 17046689]

Highlights

- Sema3F downregulates RacGTP levels in hippocampal neurons
- Sema3F activation of the RacGAP β2Chn promotes synaptic pruning *in vitro*
- β2Chn is not required for Sema3F-mediated axon repulsion or constraint of spines
- β2Chn and its GAP activity are required *in vivo* for dentate gyrus IPT axonal pruning

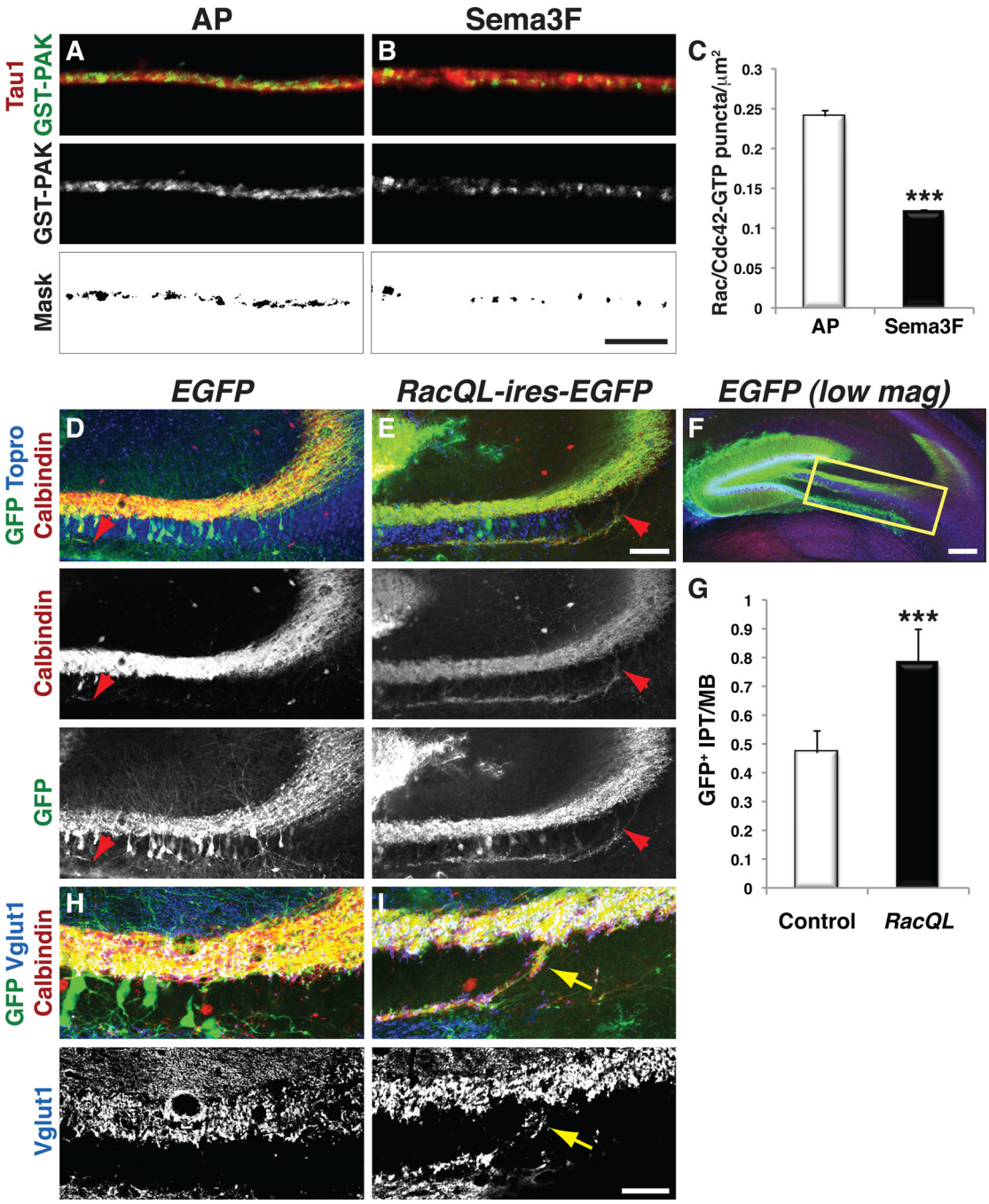

Figure 1. Down-regulation of Rac-GTP Levels is Required for Infrapyramidal Tract Pruning

(A and B) Immunostaining of DIV14 hippocampal neurons treated with 10nM AP-control (A) or Sema3F-AP (B), using GST-PAK1 (top panels, green; middle panels, white) and Tau1 (top panels, red). Bottom panels: black and white mask showing only GST-PAK1^{+} puncta in Tau1^{+} axons. Scale bar, 5μm. (C) Quantification of Rac/Cdc42-GTP puncta in hippocampal neurons presented as puncta per μm^{2} of axonal fluorescence in AP-treated (0.24±0.007 puncta/μm^{2}) and Sema3F-AP treated cultures (0.121±0.0015 puncta/μm^{2}; two tailed t-test, n=3 experiments, ***p= 0.00082). (D–F) Expression of control *EGFP* (D and F) or *RacQL-ires-EGFP* (E) from lentivirus stereotactically injected into the dentate gyrus at P20 and shown here at P45. Coronal brain sections were immunostained for calbindin

(middle panel in white, top panel red), GFP (bottom panel in white, top panel in green) and counterstained with ToproIII (top panel, blue). (E) The IPT is not pruned in the presence of constitutively active Rac. Scale bar, 100 μm. (F) GFP control lentivirus injection showing a representative region of interest magnified in (D) and (E). Red arrowheads mark the distal end of calbindin^{+}/GFP^{+} IPT fibers. Scale bar, 250 μm. (G) Quantification of the ratio of GFP^{+}, calbindin^{+} IPT length to the length of the MB in control (0.469±0.07, n=7) and *RacQL-IRES-EGFP* injected animals (0.782±0.115, n=6, two-tailed t-test: ***p= 0.00011; error bars, s.d.). (H and I) Immunostaining for vGlut1 (bottom panel white, top panel blue), calbindin (top panel, red) and GFP (top panel, green) in EGFP-expressing (H) or *RacQL-ires-EGFP*–expressing (I) lentivirus-injected DG granule cell axons extending within the IPT. Yellow arrows mark presynaptic vGlut1^{+} terminals present in *RacQL-ires-EGFP*–expressing distal IPT axons (I). Scale bar, 50 μm.

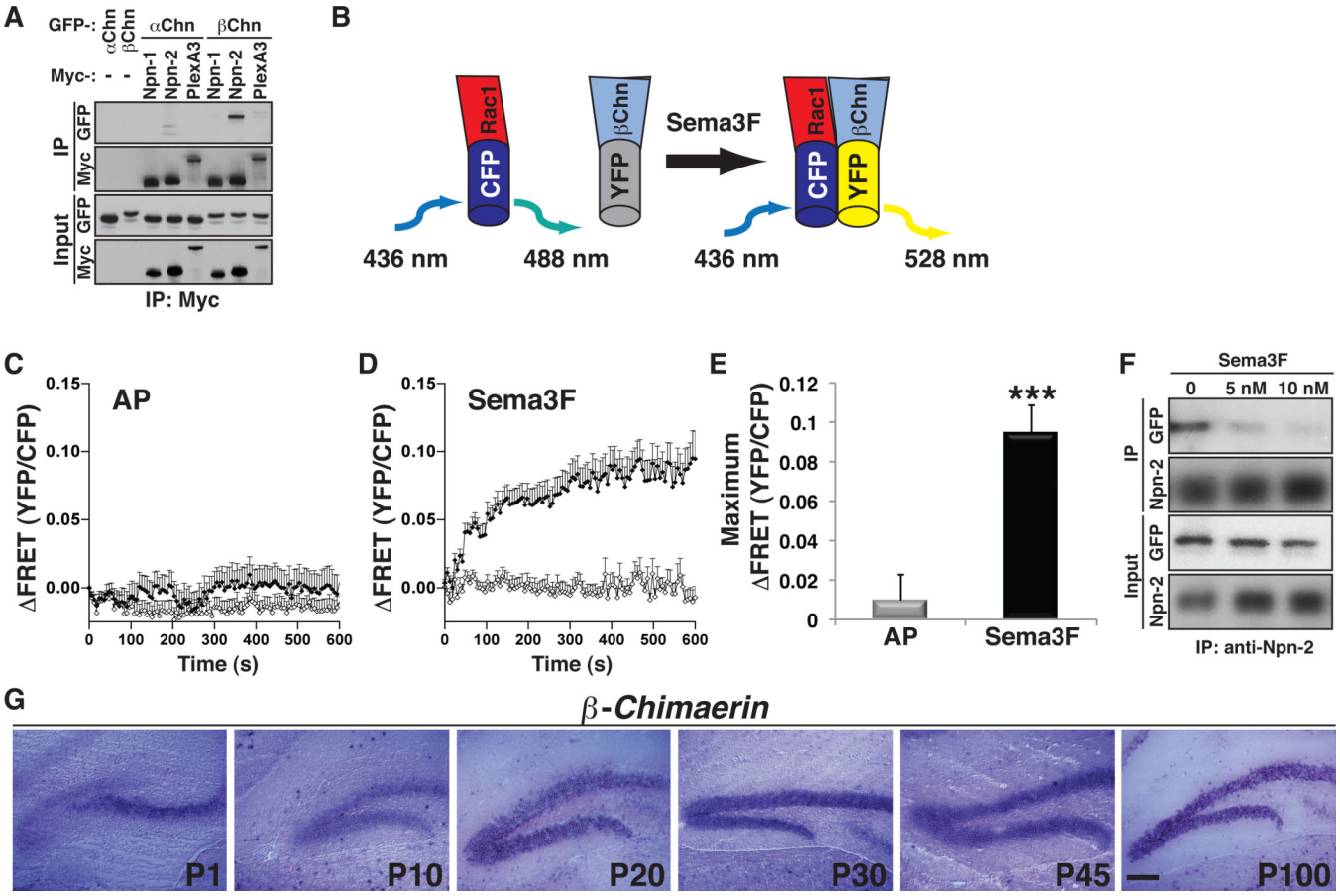

Figure 2. The Rac-GAP β2-Chimaerin Binds to Neuropilin-2 and is Activated at the Membrane by Sema3F

(A) Co-immunoprecipitation of GFP tagged chimaerins (α2Chn or β2Chn) with Myc tagged neuropilin-1 (Npn-1), neuropilin-2 (Npn-2) or plexinA3 (PlexA3) in HEK293 cells *in vitro*. Npn-1, Npn-2 and PlexA3 were immunoprecipitated with antibodies directed against the Myc tag and co-precipitation of chimaerins was detected. Note the strong interaction between β2Chn and Npn-2. (B) Schematic of FRET probes used to evaluate β2Chn activation (Wang et al., 2006). (C and D) Analysis of the β2Chn–Rac1 interaction by FRET at the membrane (full circles) or in the cytoplasm (open circles) of Neuro2A cells treated with 10 nM AP (C) or Sema3F (D). FRET was measured every 6 s after ligand treatment for 10 min. In the presence of Sema3F, a dramatic increase in FRET is observed selectively at the cell membrane, revealing that β2Chn is activated as evidenced by its binding to Rac1 and recruitment to the cell membrane. Error bars, s.e.m. (E) Quantitative analysis of maximum FRET in the peripheral region after AP or Sema3F treatment. Average Max ΔFRET: AP:0.0096±0.013; Sema3F: 0.0944±0.0141; t-test ***$p<0.0001$, n=34–37 membrane regions per treatment. Data are expressed as mean±s.e.m. (F) CoIP of endogenous Npn-2 and GFP-tagged β2Chn in Neuro2A cells in the presence of different Sema3F concentrations. Npn-2 was immunoprecipitated with anti-Npn-2 and GFP-β2Chn was detected using anti-GFP. Bath application of 5nM and 10nM Sema3F for 20 minutes causes a significant, dose-dependent, reduction in β2Chn binding to Npn-2. (G) Postnatal expression of β*Chn* in the dentate gyrus assessed by *in situ* hybridization. β*Chn* DG levels progressively increase after birth and peak during IPT pruning (P30–P45). Scale bar, 100 μm.

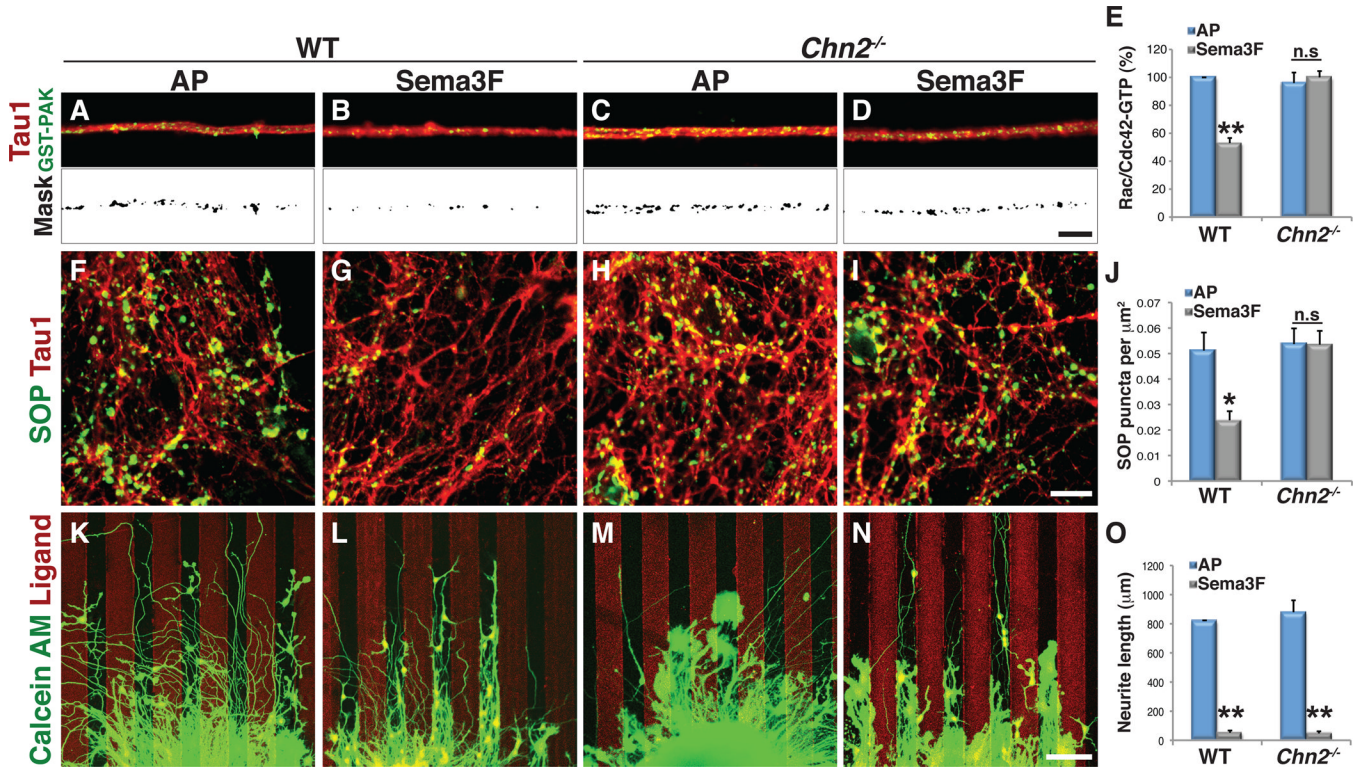

Figure 3. β2-Chimaerin is Required for Sema3F-dependent Pruning, but not Repulsion, *in vitro*

(A–D) WT (A and B) and *Chn2*$^{-/-}$ (C and D) hippocampal neurons were treated with 10nM AP (control) (A and C) or Sema3F-AP (B and D) and immunostained with GST-PAK1 (top panels, green) and with anti-Tau1 (top panels, red). Bottom panels, mask for GST-PAK1 positive puncta in axons. Scale bar, 5 µm. (E) Quantification of active Rac/Cdc42 in axons treated with AP or Sema3F expressed as a percentage of GST-PAK^{+} puncta/µm^{2} in AP-treated WT neurons (n=3, WT-AP:100%; WT-Sema3F: 52.93±3.63%; *Chn2*$^{-/-}$-AP: 95.95±7.51%; *Chn2*$^{-/-}$-Sema3F: 100.01±4.49%; ANOVA, p<0.0001, Tukey HSD Test **p<0.01. error bars, s.d.). (F–I) Synaptoporin (SOP, green) and Tau1 (red) immunolabelling of WT (F and G) and *Chn2*$^{-/-}$ (H and I) DIV21 hippocampal neurons treated with AP (F and H) or Sema3F (G and I). SOP levels are notably reduced following bath application of Sema3F to WT neurons (G), but this response is abolished in *Chn2*$^{-/-}$ neurons (I). Scale bar, 10 µm. (J) Quantification of SOP labeling assay (n=4 experiments, 10 fields per experiment, ANOVA p=0.000927, followed by Tukey HSD test, *p<0.05 compared to all other treatments; error bars, s.e.m.). WT-AP: 0.0511±0.0071; WT-Sema3F: 0.0238±0.0035; *Chn2*$^{-/-}$-AP: 0.0537±0.0062; *Chn2*$^{-/-}$-Sema3F: 0.0535 ± 0.0054 SOP puncta/µm^{2}. (K–N) Dentate gyrus explants from P2 WT (K and L) or *Chn2*$^{-/-}$ (M and N) mice were used in stripe assays with alternating AP stripes (K and M) or alternating AP and Sema3F stripes (L and N). Both WT and *Chn2*$^{-/-}$ neurites steer away from Sema3F stripes. n=16–20 explants per treatment, from 4–5 animals per genotype. Scale bar, 100 µm. (O) Quantification of neurite outgrowth performed on WT and *Chn2*$^{-/-}$ dentate gyrus explants (see Figure S4). n.s., not significant. error bars, s.e.m.

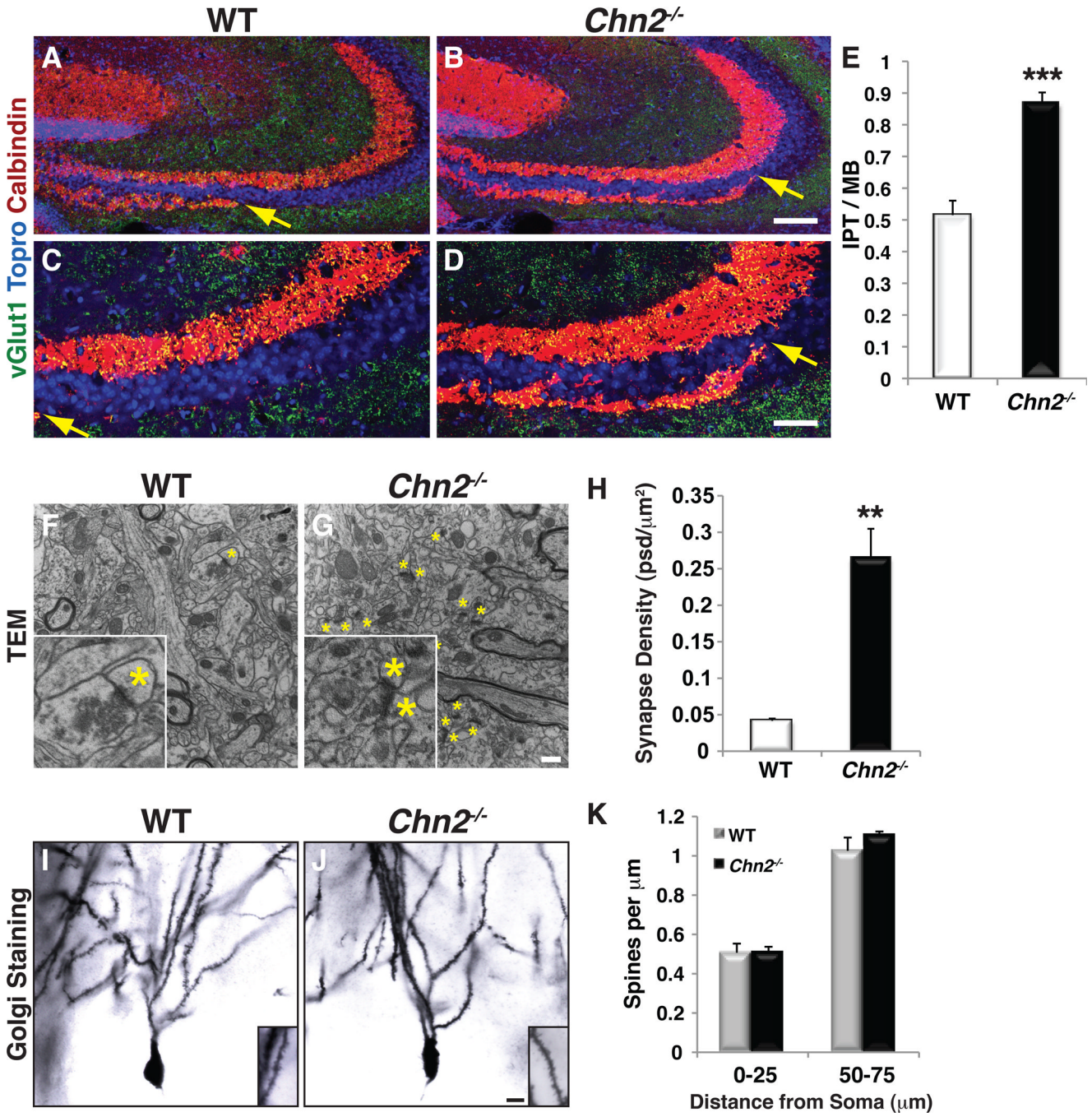

Figure 4. β2-Chimaerin is Required for IPT Pruning *in vivo*, but is Dispensable for DG Dendritic Spine Remodeling

(A–D) Immunostaining of WT (A and C) and *Chn2*$^{-/-}$ (B and D) P45 hippocampi with anti-calbindin (red), anti-vGlut1(green) and ToproIII (blue). The IPT is notably longer in *Chn2*$^{-/-}$ mice (B) compared to WT (A). Yellow arrows mark the distal end of the IPT. Scale bar, 100 μm. (C and D) Higher magnification views of (A) and (B), respectively. vGlut1^{+} presynaptic terminals are observed in the distal region of the IPT in *Chn2*$^{-/-}$ mice (D). Scale bar, 50 μm. (E) Quantification of IPT pruning, expressed as the ratio of IPT length to the length of the MB in CA3. The IPT is significantly longer in *Chn2*$^{-/-}$ mice (0.87±0.034, n=12 brain hemispheres from 8 mutant mice) than in WT (0.515±0.046, n=13 hemispheres

from 8 WT mice, two tailed t-test ***p=8.02*10^{-17}; error bars ± s.d). (F and G) Transmission electron micrographs of distal IPT regions in WT (F) and *Chn2*$^{-/-}$ (G) mice. Insets show a single axon terminal and PSD in WT (F), and a characteristic mossy fiber asymmetric synapse with two PSDs in *Chn2*$^{-/-}$ (G) mice. Asterisks mark PSDs. Scale bar, 500nm for F and G, and 150nm for insets. (H) Quantification of synapses in the distal infrapyramidal region of WT and *Chn2*$^{-/-}$ mice determined from EM analysis. WT: 0.042±0.003 psd/μm^2, *Chn2*$^{-/-}$: 0.265±0.069 psd/μm^2, two tailed t-test, t-test **p=0.005, error bars=s.e.m. (I and J) *Chn2* is not required for DG granule cell dendritic spine or anterior commissure development. Golgi staining of adult DG granule cell dendrites in WT (I) and *Chn2*$^{-/-}$ (J) hippocampi. Scale bar, 10 μm for I and J and 6 μm for insets. (K) Quantification of WT and *Chn2*$^{-/-}$ DG granule cell dendritic spine density; no significant difference between WT and *Chn2*$^{-/-}$ is observed (t-test: p=0.83 for 0–25 μm, p=0.11 for 50–75 μm; error bars ± s.d.).

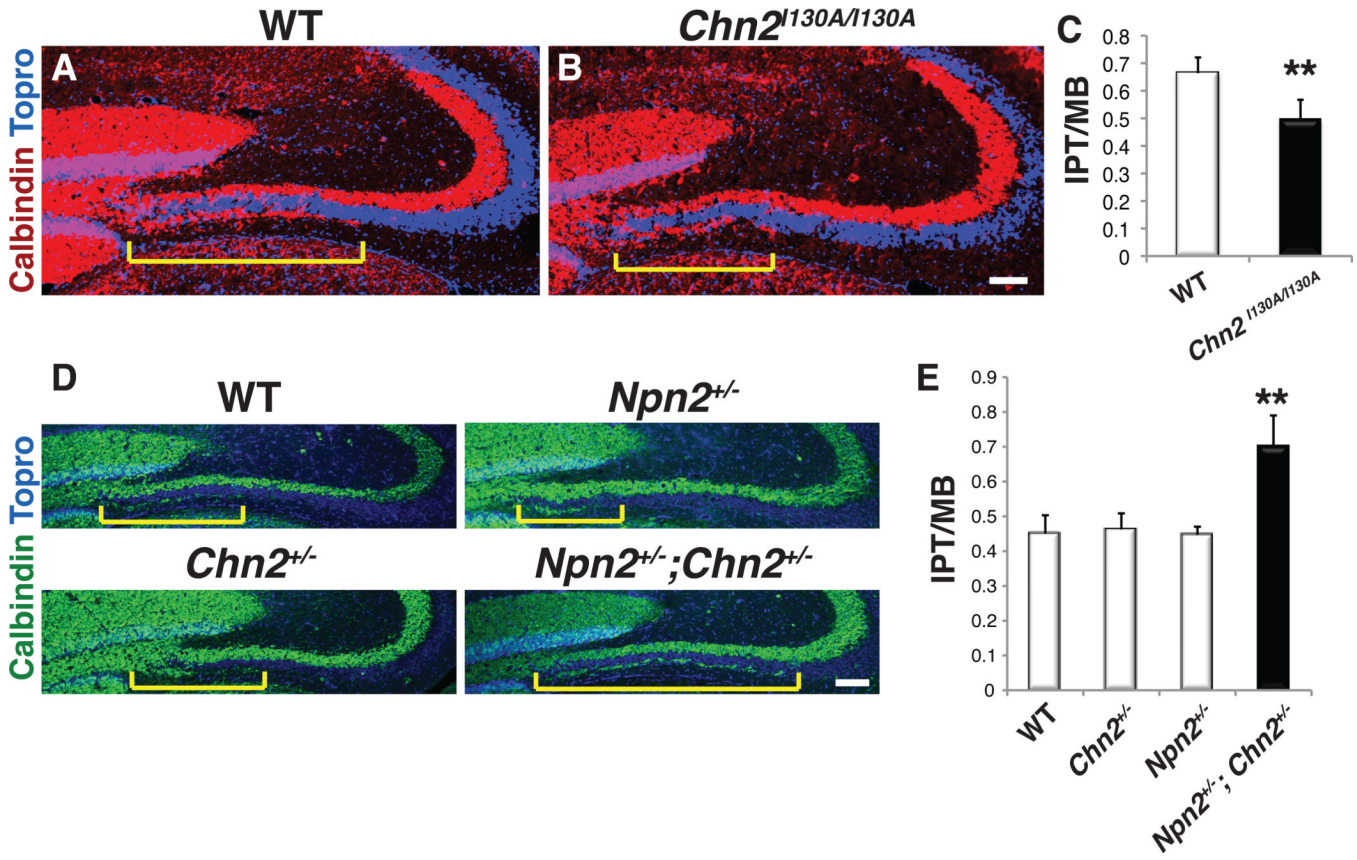

Figure 5. A Hyperactive Form of β-Chimaerin is Sufficient for IPT Pruning *in vivo*

(A and B) Immunohistochemistry with anti-calbindin (red) and ToproIII (blue) on WT and *Chn2*$^{I130A/I130A}$ P28 hippocampi. Scale bar, 100 μm. (C) Quantification of the IPT length-to-MB length ratio in WT (0.664±0.057) and *Chn2*$^{I130A/I130A}$ (KI/KI) mice (0.495±0.072, n=8, two-tailed t-test **p=0.00596). (D and E) Genetic interaction between *Npn-2* and *Chn2*. (D) Immunostaining using anti-calbindin (green) and ToproIII (blue) of WT (top left), *Npn-2*$^{+/-}$ (top right), *Chn2*$^{+/-}$ (bottom left) and *Chn2*$^{+/-}$; *Npn2*$^{+/-}$ transheterozygotes (bottom right) P45 hippocampi. Scale bar, 100 μm. (E) Quantification of the genetic interactions between *Chn2* and *Npn2* (n=7 hemispheres from 5 animals for each genotype, ANOVA p<0.0001; Tukey HSD test **p<0.01 compared to all other genotypes). WT: 0.45±0.053; *Chn2*$^{+/-}$: 0.463±0.046 ; *Npn-2*$^{+/-}$: 0.447±0.024; *Chn2*$^{+/-}$; *Npn2*$^{+/-}$: 0.698±0.092. Yellow brackets delineate IPT length in A, B, and D. error bars are s.d.

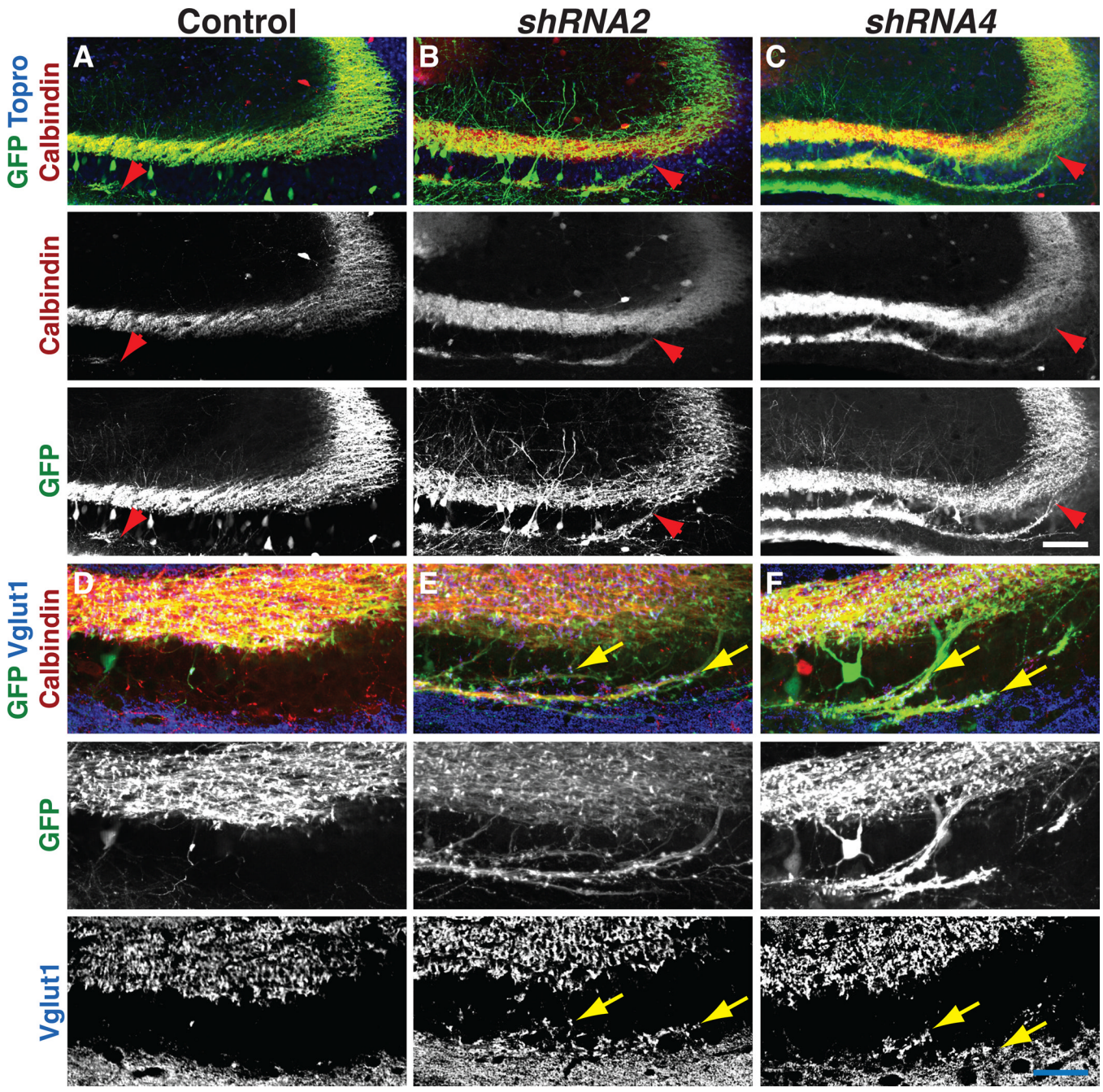

Figure 6. β2Chn is Required in the Dentate Gyrus for IPT Pruning *in vivo*. (A–C)
Histological analysis of hippocampi from control (A), *shRNA2* (B), *shRNA4* (C) lentivirus-injected animals using anti-GFP (top panels, green; bottom panels, white), anticalbindin (top panels, red; middle panels white) and ToproIII (top panels, blue). The IPT in *shRNA2*- and *shRNA4*-injected animals (B and C) extends almost as far as the distal blade of the MB, as compared to control-injected animals in which the IPT extends only 45% of the MB length (A). Arrowheads mark the distal end of the calbindin^{+}, GFP^{+} IPT fibers. Scale bar, 100μm. (D–F) β2-chimaerin is required in the dentate gyrus for IPT presynaptic pruning. Immunostaining for vGlut1 (bottom panels, white; top panel, blue), calbindin (top panels, red) and GFP (middle panels, white; top panels, green) of control (D), *shRNA2* (E),

shRNA4 (F) lentivirus-injected mice. Ectopic vGlut1$^+$ presynaptic terminals are present in the distal region of the IPT in *shRNA* injected hippocampi (E and F). Arrows point to presynaptic vGut1$^+$ terminals present in shRNA injected EGFP$^+$ distal IPT axons. Scale bar, 50 μm.

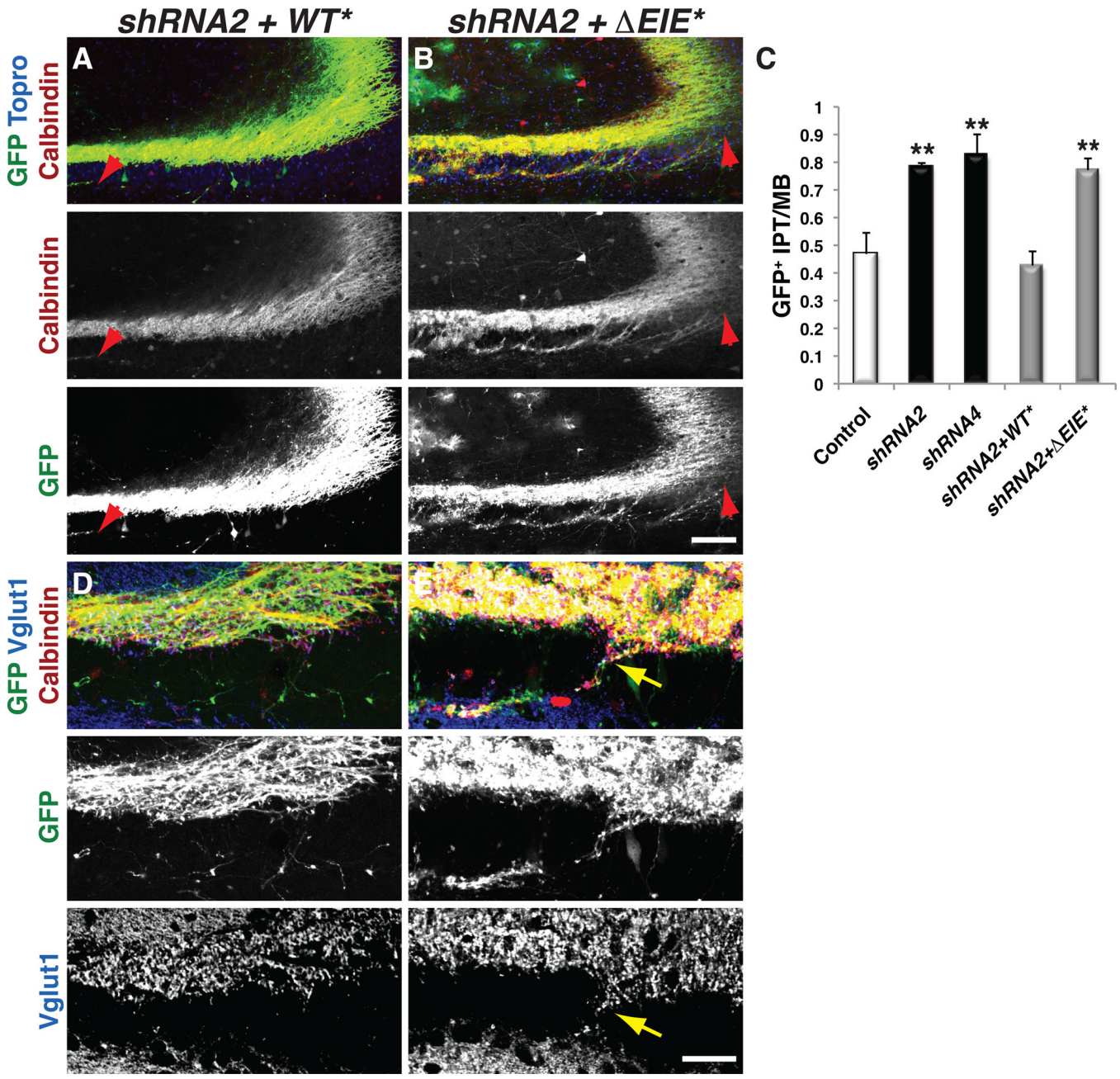

Figure 7. β2Chn GAP Function is Required in the Dentate Gyrus for IPT Pruning *in vivo*

(A and B) Immunostaining of hippocampal sections obtained from *shRNA2*+WT* (A), and *shRNA2*+Δ*EIE** (B) lentivirus-injected animals using anti-GFP (top panels, green; bottom panels, white), anti-calbindin (top panels, red; middle panels white) and ToproIII (top panels, blue). The defect observed in shRNA injected animals (see Figure 6) can be rescued by human WT β2Chn (A), but not by a human β2Chn harboring a three amino acid deletion rendering the GAP domain inactive (ΔEIE, B). Arrowheads mark the distal end of the calbindin^{+}, GFP^{+} IPT fibers. Scale bar, 100μm. (C) Quantification of GFP^{+}, calbindin^{+} IPT length expressed as a ratio of IPT/MB length. Control: 0.47±0.07, n=7; *shRNA2*: 0.78±0.013, n=6; *shRNA4*: 0.83±0.07, n=5; *shRNA2*+*WT**: 0.43±0.06, n=9; *shRNA2*+Δ*EIE**: 0.77±0.04, n=6. ANOVA ($p<0.0001$) followed by Tukey HSD test,

p<0.01 compared to control and *shRNA2+WT; error bars ± s.d. (D and E) The Rac-GAP activity of β2Chn is required in the dentate gyrus for IPT presynaptic pruning. Immunohistochemistry for vGlut1 (bottom panels, white; top panel, blue), calbindin (top panels, red) and GFP (middle panels, white; top panels, green) of *shRNA2+WT** (D), and *shRNA2+ΔEIE** (E) lentivirus-injected mice. Injection of human *shRNA*-resistant WT *β2̃Chimaerin* rescues the accumulation of vGlut1 in the distal IPT region (D), however a human GAP-deficient form of β2̃Chimaerin (ΔEIE) (E), fails to rescue the IPT pruning defect observed in *shRNA*-injected hippocampi. Arrows point to presynaptic vGut1^{+} terminals present in shRNA injected EGFP^{+} distal IPT axons (E). Scale bar, 50 μm.